

Development of double burner natural-draft biomass cookstove

S. U. Yunusa*, M. Isiaka, A. Saleh

(Department of Agricultural and Bio-resources Engineering Ahmadu Bello University, Zaria, P.M.B 1045, Kaduna State, Nigeria)

Abstract: Improved biomass cookstoves have been widely proven to be more efficient than traditional cookstoves. They are however mostly designed as single burners to utilize one fuel type. This paper presents the development of a double burner natural-draft biomass cookstove. The study conforms with the global effort of harnessing clean and efficient methods of cooking towards curtailing deforestation and mitigating the impacts of climate change. The cookstove was designed as a batch-fed double burner type with a ceramic insulated combustion chamber. The insulators were equally made detachable to ease maintenance. The cookstove was evaluated and thermal efficiency, specific fuel consumption, time spent in boiling per given weight of water, and firepower were determined. The result of the experimental analysis yielded a mean thermal efficiency ranging from 17.2% - 33.1%, mean specific fuel consumption of 0.019 - 0.089, mean time spent in boiling per given weight of water of 0.172 - 0.354 h kg⁻¹, and mean firepower of 0.458 - 3.324 kW. In line with the performance indicators, the developed cookstove was found to be energy efficient for domestic cooking with the potential to save fuel and emit less pollutants to the environment. Further studies should focus on evaluating the cookstove with other forms of biomass fuel and insulators.

Keywords: biomass, cookstove, traditional, improved, natural-draft

Citation: Yunusa, S. U., M. Isiaka, and A. Saleh. 2022. Development of double burner natural-draft biomass cookstove. *Agricultural Engineering International: CIGR Journal*, 24(2): 194-206.

1 Introduction

About three billion people in the world cook and heat their homes using various forms of biomass (Ademe, 2016). In Africa, over 82% of the population use solid biomass fuels for their primary cooking needs, however, only 11% use clean cookstoves and fuels (Boafo-mensah et al., 2020). Solapure et al. (2017) confirmed the difficulty in achieving the blue flame (complete combustion) in traditional cookstoves. The gaseous emission that emanates from traditional cookstoves' inability to completely combust fuel results in respiratory disorders and increases mortality,

especially among women (Pal, 2016; WHO, 2021). On that note, nearly 600,000 deaths and millions of chronic illnesses are recorded annually in Africa (ACCES, 2014). The effects of these emitted pollutants are enormous on the users, the environment, and the climate. Cooking was estimated to contribute about 5% of global greenhouse gas emissions (Adria and Bethge, 2013), out of which 1.9% – 2.3% are from fuelwood (Bailis et al., 2015). This implies about 2 billion tonnes of CO₂ emission per year (Adria and Bethge, 2013).

Apart from the abysmal problem of emission in the use of traditional cookstoves, fuel consumption is also of utmost concern. This contributes greatly to deforestation in many parts of the developing world as biomass resources are not sustainably harvested to meet the climate change abatement potential (Capareda, 2011; Wilson et al., 2016). Improved cookstoves are good alternatives suggested by

Received date: 2020-12-10 **Accepted date:** 2022-02-12

***Corresponding Author:** S. U. Yunusa, Department of Agricultural and Bio-resources Engineering, Ahmadu Bello University, Zaria, P.M.B. 1045, Kaduna State, Nigeria. Tel: +2348130628584. Email: suyunusa@abu.edu.ng, suleimanyunusa001@gmail.com.

many researchers as an effective approach to address the aforementioned problems. They, are solid-fuel stoves that improved on traditional baseline biomass technologies in terms of fuel efficiency and heat utilization (Thomson et al., 2016). Mehetre et al. (2017) verified that improved biomass cookstoves save up to 30% – 60% fuel and lower black carbon emissions by 50%–90%. They are designed to primarily improve fuel efficiency and minimize the emission of pollutants, thereby curtailing deforestation and climate change impacts. Agyei-Agyemang et al. (2014) also reiterated some benefits of improved cookstoves to include; improved livelihoods of its producers, health and safety benefits through the reduction of harmful gases (smoke) in homes, reduced fire risk and risk of burn injuries, fuel search and cooking time-saving, reduced fuel costs, as well encourage the use of locally manufactured technology in developing countries.

Although a plethora of improved cookstoves were developed to address the limitations of traditional cookstoves (Gumino et al., 2020), only a few were designed as multiple burners with efficient performance under natural draft. Therefore, this study aims at developing a double burner natural-draft biomass cookstove that improves fuel efficiency, heat utilization and minimizes emissions.

2 Materials and methods

2.1 Experimental site and study date

The study was conducted at the Department of Agricultural and Bio-resources Engineering, Ahmadu Bello University Zaria, Kaduna State, Nigeria. The site is located on latitude 11 °15'N to 11 °3'N of the equator and longitude 7 °30'E to 7 °45'E of Greenwich Meridian. It was conducted from 9th July to 6th August 2019.

2.2 Components design

2.2.1 Combustion chamber

2.2.1.1 Diameter of the combustion chamber (D_c)

Figure 1 shows the diameter of the combustion chamber (D_c) as indicated on the stove cap

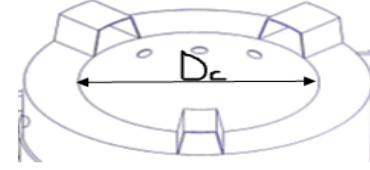


Figure 1 Stove cap indicating the diameter of the combustion chamber

The diameter of the combustion chamber (D_c) (mm) was determined from Equation 1 as given by Belonio (2005)

$$D_c = \left[\frac{1.27 \times FCR}{SGR} \right]^{0.5} \quad (1)$$

Where,

SGR = Specific gasification rate ($\text{kg m}^{-2} \text{h}^{-1}$)

FCR = Fuel consumption rate (kg h^{-1})

The energy required was determined using Equation 2 as given by Belonio (2005)

$$Q = \frac{mf \times E_s}{t} \quad (2)$$

Where,

Q = Energy required (kJ h^{-1})

mf = Mass of food (kg)

E_s = Specific energy (kJ kg^{-1})

t = Time (h)

In line with the assumption of Rupnar and Chauhan (2016), a kilogram of rice was considered to be cooked in 15 minutes (0.25 h). The specific energy of rice is about 1700 kJ kg^{-1} (Rupnar and Chauhan, 2016).

Hence,

$$Q = \frac{1 \text{ kg} \times 1700 \text{ kJ kg}^{-1}}{0.25 \text{ h}} = 6800 \text{ kJ h}^{-1}$$

FCR was determined using Equation 3 as given by Belonio (2005)

$$FCR = \frac{Q}{C \times \eta} \quad (3)$$

Where,

Q = Energy required (kJ h^{-1})

C = fuel calorific value (kJ kg^{-1})

η = Efficiency (decimal)

Since charcoal is the test fuel, its net calorific value as given by Chen et al. (2018) ($29,000 \text{ kJ kg}^{-1}$) was used,

also, assuming a minimum efficiency of cookstove to be 25% as per BIS 13152 (Part 1): 2013, we have,

$$FCR = \frac{6800 \text{ kJ h}^{-1}}{29000 \text{ kJ kg}^{-1} \times 0.25} = 0.94 \text{ kg h}^{-1}$$

SGR of Biomass material ranges between 50-210 kg m⁻² h⁻¹ (Bantelay and Gabbiye, 2014)

$$Dc = \left[\frac{1.27 \times 0.94 \text{ kJ h}^{-1}}{75 \text{ kJ m}^{-2} \text{ h}^{-1}} \right]^{0.5}$$

$$Dc = 0.126 \text{ m} = 126 \text{ mm}$$

2.2.1.2 Area of the combustion chamber

Being a cylindrical combustion chamber, the area was estimated using Bryden et al. (2002) relationship as:

$$A_C = \pi \times r_c^2 \quad (4)$$

Where,

A_C = Area of the combustion chamber (mm²)

r_c = radius of the combustion chamber (mm)

Since Dc is 126 mm, r_c will be 63 mm

$$A_C = 3.142 \times 63^2$$

$$A_C = 12,470.6 \text{ mm}^2$$

Therefore, an area of 12,470.6 mm² was used in the design of the combustion chamber.

2.2.1.3 Needed gap at the edge of the combustion chamber

Figure 2 shows the needed gap required at the edge of the combustion chamber.

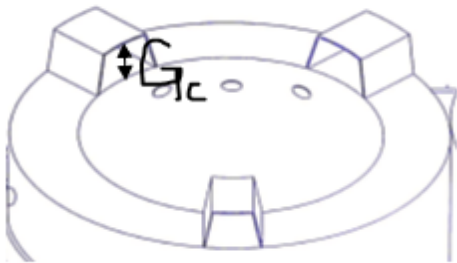


Figure 2 Stove cap showing the needed gap at the edge of the combustion chamber

This was determined from Equation 5 as given by Bryden et al. (2002)

$$G_c = \frac{A_C}{C_c} \quad (5)$$

Where,

G_c = needed gap at the edge of the combustion chamber (mm)

C_c = Circumference of the stove hot gasses outlet (mm)

$$C_c = 2 \times \pi \times r_c$$

$$C_c = 2 \times \pi \times 63 = 395.9 \text{ mm}$$

$$G_c = \frac{12,470.6}{395.9} = 31.5 \text{ mm}$$

Thus, a gap of 31.5 mm was used at the edge of the combustion chamber.

2.2.1.4 Height of the combustion chamber (H)

This was determined from Equation 6 as given by Belonio (2005)

$$H = \frac{SGR \times t}{\rho} \quad (6)$$

Where,

H = Height of combustion chamber (m)

t = Time required by the stove to operate per loading of fuel (h)

ρ = Bulk Density of fuel (kg m⁻³)

Bulk density of charcoal = 384 kg m⁻³

Assuming it takes the stove two hours to operate per loading of fuel;

$$H = \frac{75 \times 2}{384} = 0.391 \text{ m}$$

2.2.2 Total height of the stove

The total height is the sum of the height of the combustion chamber and the height above secondary airports

$$\text{Total height} = H + h \quad (7)$$

Where,

h = height above secondary airports (m)

The height above the secondary airports was taken as one-third of the total height of the combustion chamber.

$$h = H/3 \quad (8)$$

$$h = 0.391/3 = 0.130 \text{ m}$$

Hence,

$$\text{Total height of stove} = 0.391 + 0.130 = 0.521 \text{ m} = 521 \text{ mm}$$

2.2.3 Amount of air needed (AFR)

The amount of air required for combustion of fuel material was determined from Equation 9 as given by Belonio (2005).

$$AFR = \frac{\varepsilon \times FCR \times SA}{\rho} \quad (9)$$

Where,

SA = Stoichiometric air of biomass = 6 (Keche et al., 2013)

ε = Equivalence ratio = 0.3 (Keche et al., 2013)

ρ = Air density = 1.225 kg m^{-3} at 25°C (Rupnar and Chauhan, 2016)

$$AFR = \frac{0.3 \times 0.94 \times 6}{1.225} = 1.38 \text{ m}^3 \text{ h}^{-1}$$

2.2.4 Area required for primary air

The area required for the desired amount of airflow rate was computed using Equation 10 as given by Belonio (2005)

$$A = \frac{AFR}{V} \quad (10)$$

Where, V = velocity of air, m s^{-1} (indoor air velocity = $0.5 \text{ m s}^{-1} = 1800 \text{ m h}^{-1}$) as used by Rupnar and Chauhan (2016)

Hence,

$$A = \frac{1.38}{1800} = 0.000767 \text{ m}^2$$

2.2.5 Design of insulation thickness

The critical radius of insulation was determined from Equation 11 as used by Omini (2018).

$$r_c = \frac{k}{h_c} \quad (11)$$

Where,

r_c = the critical radius of insulation (m)

K = thermal conductivity of insulation material ($\text{W m}^{-1} \text{ }^\circ\text{C}^{-1}$) = $0.15 \text{ W m}^{-1} \text{ }^\circ\text{C}^{-1}$ for clay (Castaner et al., 2017).

h_c = the convective heat transfer coefficient ($\text{W m}^{-2} \text{ }^\circ\text{C}^{-1}$)

The convective heat transfer coefficient (h) was computed from Equation 12 as used by Kulla (2011)

$$h_c = 1.42 \left\{ \frac{\Delta t}{L} \right\}^{1/4} \quad (12)$$

Where,

$\Delta t = T_i - T_a$ = Change in temperature between the internal temperature ($T_i = 1100^\circ\text{C}$ (GACC, 2017)) and ambient temperature (T_a) of the combustion chamber.

$$\Delta t = 1100^\circ\text{C} - 34.6^\circ\text{C} = 1065.4^\circ\text{C}$$

L = Length of the combustion chamber, m

The length of the combustion chamber was determined from Equation 13 as used by Kulla (2011)

$$L \approx 3 \times D_c \quad (13)$$

Where,

D_c = diameter of the combustion chamber, m

$$L = 3 \times 0.126 = 0.378 \text{ m}$$

$$h_c = 1.42 \left\{ \frac{1065.4}{0.378} \right\}^{1/4} = 10.35 \text{ W m}^{-2} \text{ }^\circ\text{C}^{-1}$$

$$r_c = \frac{0.15}{10.35} = 0.0145 \text{ m}$$

2.3 Isometric view of the cookstove

The isometric view of the cookstove is shown in Figure 3.

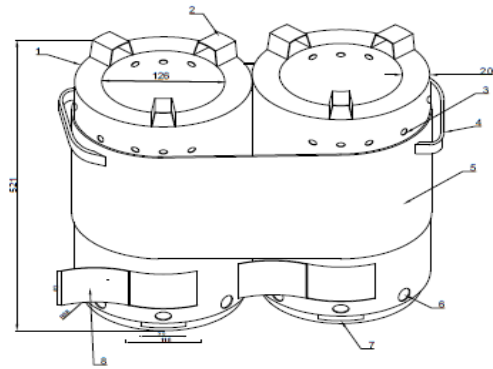


Figure 3 Isometric view of the cookstove

2.4 Description of the developed cookstove

The developed prototype is a batch-fed natural draft cookstove which was made with a double burner to fast-track the cooking process. It comprises a heat-resistant handle, insulated grate, a detachable refractory lining, air inlets, an ash deposit chamber, and a cap comprising of a pot seat.

The pictorial view is shown in Figure 4 and 5.



Figure 4 Cookstove pictorial view



Figure 5 Cookstove top view

2.5 Experimental setup and data collection

The performance indicators (thermal efficiency, specific fuel consumption, time spent in boiling per given weight of water and firepower) were determined by considering the independent variables; fuel quantity **F**, air inflow rate **A**, and fuel size **S**. The experiment was conducted using Completely Randomized Design (CRD) at three (3) levels of fuel quantity (filled F1 = 890 g and 810 g, half-filled F2 = 445 g and 405 g, and two-thirds filled fuel space F3 = 593 g and 540 g) using two (2) fuel sizes (coarse sizes S1 = 5-15 cm long and small sizes S2 = 1- 5 cm long), respectively. Three (3) levels of air inflow rate (maximum A1 = 0.3 m s^{-1} , moderate A2 = 0.2 m s^{-1} , and minimum A3= 0.1 m s^{-1}) were equally considered. The experiment was replicated thrice. Statistical Analysis System (SAS) software was employed for the analysis and Duncan Multiple Range Test (DMRT) was used to further analyze the significant variables.

The stove was evaluated using the standard Water Boiling Test (WBT) Version 3.0 as suggested by Bailis et al. (2007). The test which was an open lid experiment was conducted in a well-ventilated laboratory with an average air temperature and relative humidity of 27°C and 75.6%, respectively. The test has two (2) experimental phases; the high-power phase (cold and hot start) and the low power phase (simmering). Charcoal was used as the test fuel and its moisture content (7.8% wet basis) was determined using the standard oven-dry test.

On evaluation, two (2) aluminum pots tagged pot 1 and 2 as shown in Figure 6, with capacities of 4.4 and 4.9 liters, respectively were used for the test. Water volume, two-thirds of the pot's capacities (i.e., 2.93 and 3.3 liters) were used. The pots were filled to stated capacities and weighed before and after each test phase. About 15ml of paraffin oil was sprinkled on the charcoal surface to initiate combustion. The initial and final water temperatures were noted in each test phase with the aid of mercury-in-glass thermometer held in a wooden fixture, 5 cm above the base of the pots as shown in Figure 6, and an infrared thermometer. The level of temperature increase was recorded at an interval of 5 minutes to boiling temperature.

The experimental setup is shown in Figure 6.



Figure 6 Experimental Setup

2.6 Instrumentation

The equipment used in evaluating the performance of the cookstove are as follows:

A Camry digital weight balance, model EK5350; with a sensitivity of 0.1 g and a maximum capacity of 5kg/11lb was used for measuring the weight of fuel and water

1) 2 mercury in glass thermometers (100°C capacity) were employed for measuring the water temperature variation at an interval of 5 minutes to boiling point

2) 1x2x24" wooden fixture with thermometer housing was used to hold the thermometers in the pots.

3) Infra-red thermometer, model AR852B+ (-50°C-700°C) was used in measuring the initial water temperature and to verify initial readings of the mercury in glass thermometers before steaming

4) Digital stopwatch with a sensitivity of 0.01 sec accuracy was used for timing the duration of boiling

5) 2 Aluminum pots with capacities of 4.4 and 4.9 liters were used as the experimental test-pots

6) Smart sensor AR837, was used to measure ambient humidity and temperature

7) 1000ml capacity measurement cylinder was used for water measurement

8) Digital anemometer model AM-4220 AC55807 was used for airspeed measurement

9) A metallic tong was used for handling and maneuvering the combusting fuel

10) A metal tray was used to hold charcoal for weighing

11) Heat resistant pad was used to protect the scale.

3 Results and discussion

3.1 Result of thermal efficiency

3.1.1 Interaction effects on thermal efficiency at cold start

The interaction effect of fuel quantity, air inflow rate, and fuel size on thermal efficiency at cold start is shown in Table 1. In this phase, an efficiency of 0.331 (33.1%) was observed as the best and equally the overall best when compared with other experimental phases. As depicted in Figure 4, the value (0.331) was noted at two-thirds filled (F3) fuel capacity in interaction with coarse fuel sizes (S1) under maximum air inflow (A1). In this interaction, the combustion chamber was neither filled to the brim nor left maximumly for air. It was, however, fed at an optimum of two-thirds capacity with one-third air space for effective combustion. Thus, the fuel-air ratio yielded a good radiative heat transfer from the combustion chamber to the pot. The value obtained (33.1%) agrees with BIS 13152 test code (Part 1): 2013, Kulla (2011) and Komolafe and Awogbemi (2010). The lowest mean thermal efficiency of 0.183 (18.3%) was, however, observed when the fuel space was half-filled (F2) with coarse fuel sizes (S1) under moderate

air inflow (A2).

Table 1 Interaction effect of fuel quantity, air inflow rate, and fuel size on thermal efficiency at high power cold start phase

Treatment	Mean thermal efficiency (Decimal)									
	Fuel Quantity (F)									
Air inflow rate (A)	F1			F2			F3			
Fuel Size (S)	A1	A2	A3	A1	A2	A3	A1	A2	A3	
S1	0.235ef	0.210hi	0.195ij	0.211h	0.183j	0.189j	0.331a	0.304b	0.195ij	
S2	0.227efg	0.241e	0.217gh	0.234ef	0.233ef	0.186j	0.269c	0.224fgh	0.253d	
SE ±				0.0055						

Note: Mean followed by the same letter(s) in the same column and row are not different statistically at $p=0.05$ using DMRT

3.1.2. Interaction effect on thermal efficiency at the hot start and simmering phase

Table 2 shows the result of thermal efficiency at the hot start phase. In this phase, as shown in Figure 7, an efficiency of 0.323 (32.3%) was observed to be the highest at two-thirds filled (F3) coarse (S1) fuel capacity, under a maximum air inflow (A1). This conforms to the values recorded by Bofo-Mensah et al. (2013), Kulla (2011), and Komolafe and Awogbemi (2010). However, as indicated in Figure 7, thermal efficiency of 0.172 (17.2%) was observed at half-filled (F2) coarse fuel size (S1) capacity, under minimum air inflow (A3) as the overall least thermal efficiency when compared with other experimental phases. This was attributed to the imbalance in fuel-air interaction, which resulted in increased fuel consumption, low heat utilization, and consequently a lower efficiency.

Table 3 shows the result of thermal efficiency at the simmering phase. In this phase, as indicated in Figure 7, a thermal efficiency of 0.302 (30.2%) was attained as the highest at two-thirds filled (F3) coarse fuel (S1) capacity under maximum air inflow (A1). Although the observed value is lower than that of the cold start phase, it is still higher than the value reported by Rupnar and Chauhan (2016) and agrees with the range of values reported by

Kulla (2011).

Table 2 Interaction effect of fuel quantity, air inflow rate, and fuel size on thermal efficiency at high power hot start phase

Mean thermal efficiency (Decimal)									
Treat ment	Fuel Quantity (F)								
Air inflow rate (A)	F1			F2			F3		
Fuel Size (S)	A1	A2	A3	A1	A2	A3	A1	A2	A3
S1	0.19 2fg	0.19 3efg	0.18 0h	0.20 0def	0.19 7efg	0.1 72h	0.3 23a	0.24 8b	0.19 4efg
S2	0.20 1def	0.20 5de	0.21 2cd	0.18 7g	0.22 1c	0.1 86g	0.2 57b	0.20 4def	0.25 4b
SE ±	0.0043								

Note: Mean followed by the same letter(s) in the same column and row are not different statistically at P=0.05 using DMRT

Table 3 Interaction effect of fuel quantity, air inflow rate, and fuel size on thermal efficiency at low power simmering phase

Mean thermal efficiency (Decimal)									
Treat ment	Fuel Quantity (F)								
Air inflow rate (A)	F1			F2			F3		
Fuel Size (S)	A1	A2	A3	A1	A2	A3	A1	A2	A3
S1	0.24 6c	0.225 defg	0.22 2efg	0.174 i	0.23 9cde	0.1 93h	0.30 2a	0.2 74b	0.235 cdef
S2	0.24 1cd	0.265 b	0.23 7cde	0.231 cdef	0.23 7cde	0.2 00h	0.20 8gh	0.2 03h	0.219 fg
SE ±	0.0061								

Note: Mean followed by the same letter(s) in the same column and row are not different statistically at P=0.05 using DMRT

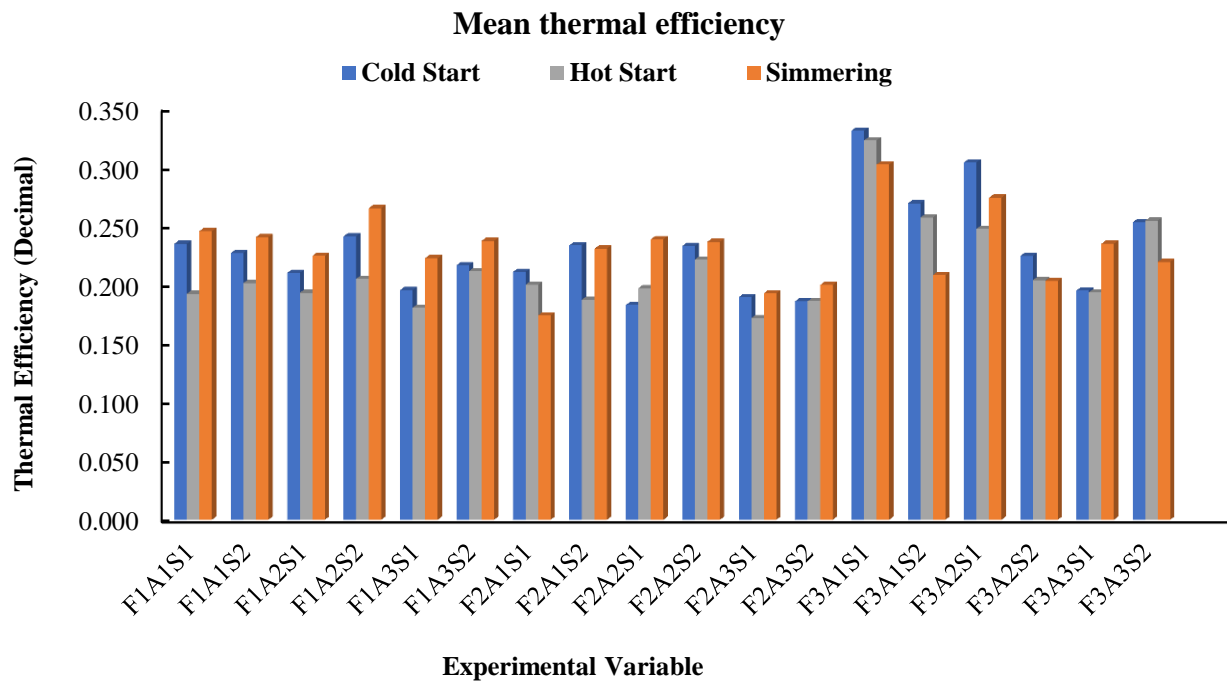


Figure 7 Mean thermal efficiency of all experimental unit

3.2 Result of specific fuel consumption (SFC)

3.2.1 Interaction effects on specific fuel consumption at cold start

Table 4 shows the interaction effect of fuel quantity, air inflow rate, and fuel size on specific fuel consumption at cold start. In this phase, the lowest (best) SFC was observed when the fuel space was two-thirds filled (F3) with coarse fuel sizes (S1) under a maximum air inflow (A1) as 0.045. However, when compared with other experimental phases

as shown in Figure 8, the overall highest SFC was recorded as 0.089 when the fuel unit was filled (F1) with coarse fuel sizes (S1) under maximum air inflow (A1). This conforms to the value obtained by Saiyyadjilani et al. (2018). And is mainly because at cold start, the cookstove ignites at room temperature, hence, a higher draft was observed, and consequently contributed to the overall fuel consumption.

3.2.2 Interaction effects on specific fuel consumption at the hot start and simmering phase

Table 5 shows the interaction between the fuel quantity, air inflow rate, and fuel size at the hot start phase. Similar to the previous phase, the lowest (best) SFC was observed as 0.049 when the fuel space was two-thirds filled with coarse fuel sizes under maximum air inflow (A1) and the highest (least) was recorded as 0.088 when the fuel space was filled (F1) with coarse fuel sizes and operated under maximum air inflow (A1).

Table 4 Interaction effect of fuel quantity, air inflow rate, and fuel size on specific fuel consumption at high power cold start phase

Specific Fuel Consumption									
Treat ment	Fuel Quantity (F)								
Air inflow rate (A)	F1			F2			F3		
Fuel Size (S)	A1	A2	A3	A1	A2	A3	A1	A2	A3
S1	0.08 9a	0.08 6a	0.07 5bc	0.07 6bc	0.07 5bc	0.06 3d	0.04 5e	0.05 9d	0.07 6bc
S2	0.07 4bc	0.08 6a	0.08 2ab	0.06 8cd	0.06 4d	0.07 5bc	0.06 1d	0.07 5bc	0.07 5bc
SE ±	0.0035								

Note: Mean followed by the same letter(s) in the same column and row are not different statistically at P=0.05 using DMRT

Table 5 Interaction effect of fuel quantity, air inflow rate, and fuel size on specific fuel consumption at high power hot start phase

Specific Fuel Consumption									
Treat ment	Fuel Quantity (F)								
Air inflow rate (A)	F1			F2			F3		
Fuel Size (S)	A1	A2	A3	A1	A2	A3	A1	A2	A3
S1	0.08 8a	0.085 abc	0.08 1b-e	0.05 9m	0.07 4f-i	0.07 4f-i	0.04 9n	0.07 7d-g	0.08 7ab
S2	0.08 0c-f	0.066 kl	0.06 7j-l	0.06 8i-k	0.08 3a-d	0.07 6e-h	0.06 1lm	0.07 3g-j	0.07 0h-k
SE ±	0.0024								

Note: Mean followed by the same letter(s) in the same column and row are not different statistically at P=0.05 using DMRT

Table 6 shows the DMRT test on the second level of interaction between the fuel quantity, air inflow rate, and fuel size at the simmering phase. In this phase, as shown in Figure 8, the overall best (lowest) SFC of 0.019 was

observed. This was achieved at half-filled (F2) small sizes fuel (S2) capacity under moderate air inflow (A2). Although Sood et al. (2018) and Saiyyadjilani et al. (2018) obtained a good SFC value, the value recorded in this phase is better. This was mainly because the simmering phase is a low power phase that simmers water at very low fuel consumption.

Table 6 Interaction effect of fuel quantity, air inflow rate, and fuel size on specific fuel consumption at low power simmering phase

Specific Fuel Consumption									
Treat ment	Fuel Quantity (F)								
Air inflow rate (A)	F1			F2			F3		
Fuel Size (S)	A1	A2	A3	A1	A2	A3	A1	A2	A3
S1	0.02 8def	0.03 6bcd	0.04 2ab	0.02 3efg	0.02 8def	0.02 5efg	0.02 2fg	0.03 7bc	0.04 6a
S2	0.02 5efg	0.03 7bc	0.03 4bcd	0.02 2fg	0.01 9g	0.03 7bc	0.03 4bcd	0.03 0c-f	0.03 1cde
SE ±	0.0029								

Note: Mean followed by the same letter(s) in the same column and row are not different statistically at P=0.05 using DMRT

3.3 Result of time spent in boiling per given weight of water

3.3.1 Interaction effects on time spent in boiling per given weight of water at cold start

Table 7 shows the result of the second level interaction between fuel quantity, air inflow rate, and fuel size on the time spent in boiling per given weight of water at the cold start phase. As shown in Figure 9, the overall best (lowest) time spent in boiling when compared to other phases, was observed in this phase as 0.172 h kg⁻¹, at coarse (S1) filled fuel space (F3) under maximum air inflow (A1). The percentage of heat utilized in this phase was high, at such heat loss was curtailed and consequently boiling was achieved within a short period.

The highest, on the other hand, was noted when the fuel space was filled (F1) with coarse fuel sizes (S1) at moderate air inflow (A2) as 0.301 h kg⁻¹. This was attributed to the poor air intake in the combustion chamber as it was relatively void of air space. The recorded value is in

agreement with Bello et al. (2015) who recorded 0.36 h kg⁻¹ who obtained 0.66 h kg⁻¹. and better than that of Komolafe and Awogbemi (2010)

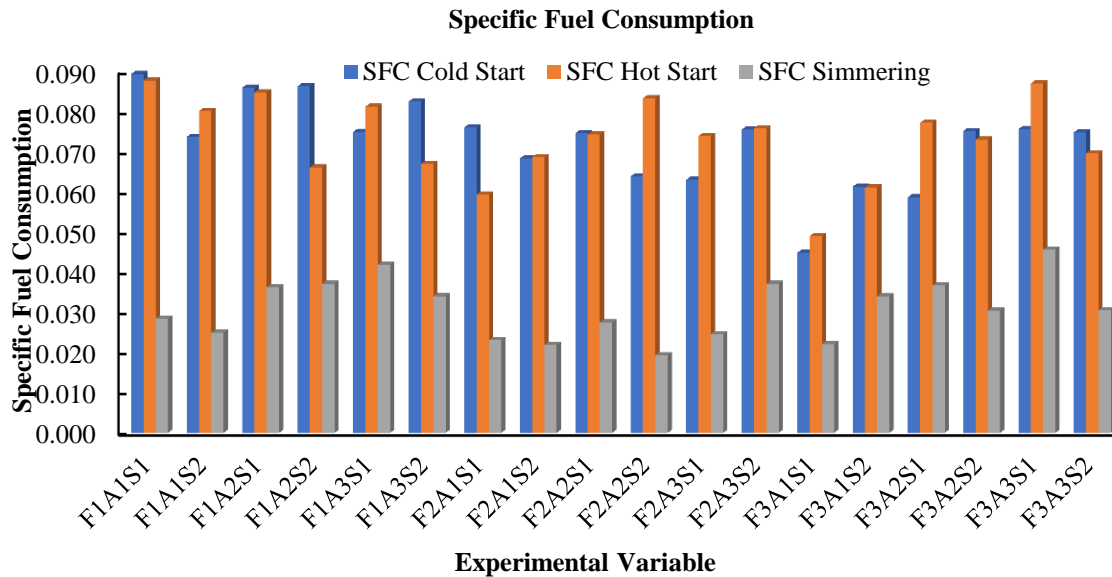


Figure 8 Mean specific fuel consumption of all experimental unit

Table 7 Interaction effect of fuel quantity, air inflow rate, and fuel size on time spent in boiling per given weight of water at high power cold start phase

Time spent in boiling per given weight of water (h/kg)									
Treatment		Fuel Quantity (F)							
Air inflow rate (A)		F1			F2			F3	
Fuel Size (S)	A1	A2	A3	A1	A2	A3	A1	A2	A3
S1	0.251b	0.301a	0.219def	0.224def	0.267b	0.175h	0.172h	0.184h	0.236cde
S2	0.238bcd	0.250bc	0.312a	0.208fg	0.239bcd	0.199g	0.184h	0.214efg	0.250bc
SE ±	0.0081								

Note: Mean followed by the same letter(s) in the same column and row are not different statistically at P=0.05 using DMRT

3.3.2. Interaction effects on time spent in boiling per given weight of water at the hot start and simmering phase

boiling at the hot start phase. Similar to the cold start phase, 0.173 h kg⁻¹ was recorded as the best (lowest) at half-filled (F2) coarse (S1) fuel capacity under maximum air inflow (A1).

Table 8 shows the effect of interaction between fuel quantity, air inflow rate, and fuel size on time spent in

Table 8 Interaction effect of fuel quantity, air inflow rate, and fuel size on time spent in boiling per given weight of water at high power hot start phase

Time spent in boiling per given weight of water (h kg-1)									
Treatment		Fuel Quantity (F)							
Air inflow rate (A)		F1			F2			F3	
Fuel Size (S)	A1	A2	A3	A1	A2	A3	A1	A2	A3
S1	0.263bc	0.275b	0.225e	0.173h	0.262bc	0.221ef	0.237de	0.187gh	0.311a
S2	0.239de	0.230de	0.175h	0.204fg	0.321a	0.237de	0.245cd	0.274b	0.275b
SE ±	0.0064								

Note: Mean followed by the same letter(s) in the same column and row are not different statistically at P=0.05 using DMRT

In Table 9, the highest time spent in boiling was recorded as 0.354 h kg⁻¹ when the fuel space was two-thirds filled (F3) with coarse fuel (S1) at minimum air inflow

(A3). As shown in Figure9, in comparison with other experimental phases, 0.354 h kg⁻¹ is the highest time recorded to reach boiling. Contrary to cold and hot start

phases, where boiling was achieved in less than 45 minutes, the simmering phase was generally designed to simmer water for 45 minutes at a temperature just below boiling. Thus, a higher value was observed in this phase. The

recorded value conforms with the value observed by Bello et al. (2015) as 0.36 h kg⁻¹ and slightly better than that of Komolafe and Awogbemi (2010) as 0.66 h kg⁻¹.

Table 9 Interaction effect of fuel quantity, air inflow rate, and fuel size on time spent in boiling per given weight of water at low power simmering phase

Treatment		Time spent in boiling per given weight of water (h/kg)								
		Fuel Quantity (F)								
Air inflow rate (A)		F1			F2			F3		
Fuel Size (S)		A1	A2	A3	A1	A2	A3	A1	A2	A3
S1		0.336b	0.340b	0.335b	0.273g	0.294e	0.318c	0.333b	0.317cd	0.354a
S2		0.288ef	0.335b	0.290ef	0.281fg	0.340b	0.306d	0.299e	0.298e	0.299e
SE ±		0.0042								

Note: Mean followed by the same letter(s) in the same column and row are not different statistically at P=0.05 using DMRT

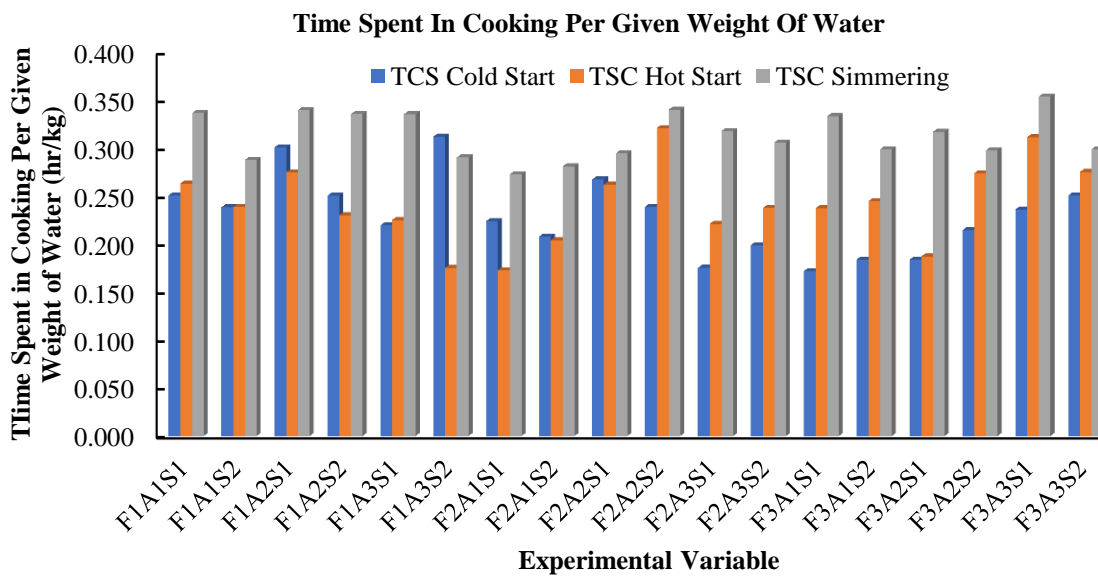


Figure 9 Mean time spent in cooking per given weight of water at different experimental unit

3.4 Result of firepower

3.4.1 Interaction effects on firepower at cold start

Table 10 shows the result of the second level interaction between fuel quantity, air inflow rate, and fuel size on firepower at cold start. As shown in Figure 10, the highest mean firepower in this phase was observed as 3.117 kW at

half-filled (F2) fuel space with small fuel sizes (S2) under minimum air inflow (A3). This agrees with the value obtained by Kumar and Panwar, (2019) (3.15 kW), and is better than that of Usman (2011), and Patil et al. (2017) who recorded 7.59 kW, and 4.48 kW, respectively.

Table 10 Interaction effect of fuel quantity, air inflow rate, and fuel size on firepower at high power cold start phase

Treatment		Fire Power (kW)								
		Fuel Quantity (F)								
Air inflow rate (A)		F1			F2			F3		
Fuel Size (S)		A1	A2	A3	A1	A2	A3	A1	A2	A3
S1		2.870ab	2.310e-h	2.759b-f	2.757a-d	2.248fgh	2.889ab	2.103h	2.572b-f	2.579a-d
S2		2.486c-g	2.778a-d	2.130gh	2.646b-e	2.153gh	3.117a	2.685b-e	2.824abc	2.405d-h
SE ±		0.0042								

Note: Mean followed by the same letter(s) in the same column and row are not different statistically at P=0.05 using DMRT

3.4.2 Interaction effects on firepower at the hot start and simmering phase

Table 11 shows the interaction effect of fuel quantity, air inflow rate, and fuel size on firepower at the hot start phase. Here, as shown in Figure 10, the overall power rating

of 3.324 kW was obtained. This was observed when the fuel space was at two-thirds filled (F3) capacity with coarse fuel sizes (S1) under moderate air inflow (A2). The recorded result was attributed to the fact that fuel combustion was at high power.

Table 11 Interaction effect of fuel quantity, air inflow rate, and fuel size on firepower at high power hot start phase

Fire Power (kW)										
Treatment		Fuel Quantity (F)								
Air inflow rate (A)		F1			F2			F3		
Fuel Size (S)		A1	A2	A3	A1	A2	A3	A1	A2	A3
S1		2.702cd	2.485de	2.911bc	2.766cd	2.285efg	2.699cd	1.662h	3.324a	2.252efg
S2		2.705cd	2.315def	3.077ab	2.708cd	2.091fg	2.608d	2.012g	2.148fg	2.037g
SE ±						0.1028				

Note: Mean followed by the same letter(s) in the same column and row are not different statistically at P=0.05 using DMRT

In Table 12, the highest firepower (1.038 kW) was recorded when the fuel space was 2/3 filled (F3) with coarse fuel sizes (S1) at a minimum air inflow rate (A3), while the least mean firepower which is the overall best (lowest) was recorded as 0.458 kW at half-filled (F3) small fuel sizes

(S2) capacity under moderate air inflow (A2). Although Odesola and Kazeem (2014) obtained lower values of 1.40 - 1.66 kW, the recorded value in this phase is better than theirs.

Table 12 Interaction effect of fuel quantity, air inflow rate, and fuel size on firepower at low power simmering phase

Fire Power (kW)										
Treatment		Fuel Quantity (F)								
Air inflow rate (A)		F1			F2			F3		
Fuel Size (S)		A1	A2	A3	A1	A2	A3	A1	A2	A3
S1		0.680def	0.859a-d	1.002ab	0.680	0.752cde	0.622efg	0.533f	0.931abc	1.038a
S2		0.698def	0.891abc	0.942ab	0.627efg	0.458g	0.967ab	0.917ab	0.823bcd	0.823bcd
SE ±						0.0662				

Note: Mean followed by the same letter(s) in the same column and row are not different statistically at P=0.05 using DMRT

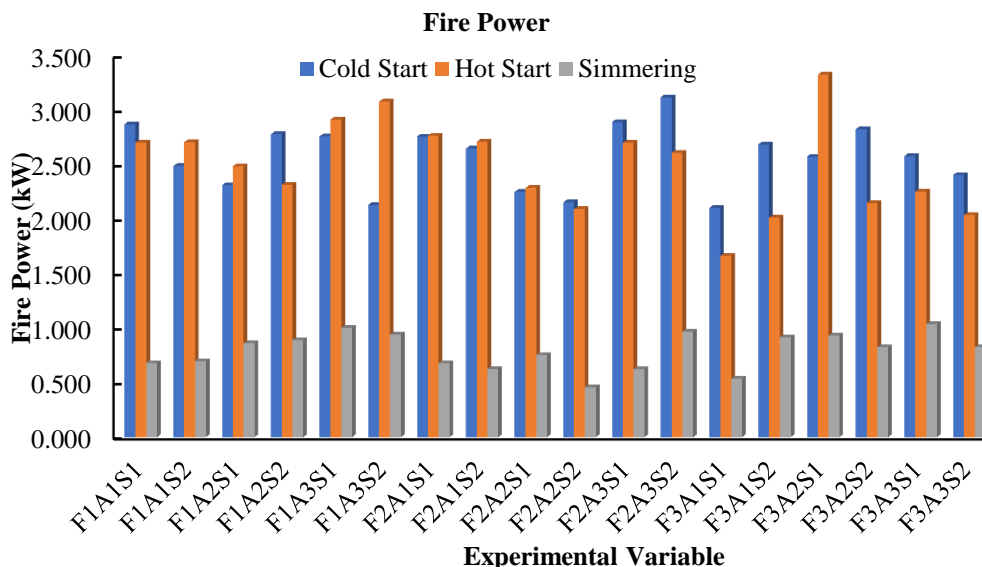


Figure 10 Mean firepower at different experimental unit

4 Conclusion

A double burner natural-draft biomass cookstove was developed. The cookstove was designed and fabricated with an overall height, diameter, and insulation thickness of 521 mm, 126 mm, and 14.5 mm, respectively. The prototype was evaluated using the standard water boiling test version 3.0 and the thermal efficiency, specific fuel consumption, time spent in boiling per given weight of water, and firepower were estimated.

On evaluation, the cookstove revealed the best thermal efficiency and time spent in boiling per given weight of water in the cold start phase at two-thirds filled coarse fuel capacity under maximum air inflow (F3A1S1) as 33% and 0.172 h kg^{-1} ($10.32 \text{ min kg}^{-1}$), respectively. However, the best (lowest) specific fuel consumption and firepower were observed in the simmering phase as 0.019 and 0.458 kW, respectively.

With an overall thermal efficiency of 33%, the cookstove meets the tier 2 to 3 category, which is uncommon in natural draft cookstoves. Hence, the developed cookstove is recommended for domestic use over the traditional cookstoves, however, future studies would involve evaluating the cookstove with other forms of biomass fuels and heat insulators as well as upgrading to force convection to suit environments with low airspeed.

Acknowledgment

The authors gratefully acknowledge the Institute for Agricultural Research (IAR), Ahmadu Bello University, Zaria, Nigeria for funding the research.

References

- Ademe, R. 2016. Easing women's life with energy efficient cook stove. World Vision Report. Sub-City; Kebele 11, Addis Ababa, Ethiopia: World Vision Ethiopia. Retrieved from www.wvi.org/ethiopia
- Adria, O., and J. Bethge. 2013. What users can save with energy-efficient cooking stoves and ovens. Wuppertal, Germany: Wuppertal Institute for Climate, Environment and Energy, Germany.
- Africa Clean Cooking Energy Solution Initiative (ACCES). 2014. Clean and improved cooking in Sub-Saharan Africa. A landscape report. 2nd ed. Washington, D.C., USA: the World Bank.
- Agyei-Agyemang, A., P. O. Tawiah, and F. Nyarko. 2014. Efficient charcoal stoves: enhancing their benefits to a developing country using an improved design approach. *International Journal of Engineering Trends and Technology*, 15(2): 94-100.
- Bailis, R., D. Ogle, N. MacCarty, and D. Still. 2007. The water boiling test (WBT) version 3.0 for the household energy and health programme. Household Energy and Health Programme, Shell Foundation: Shell Centre, London, SE1 7NA, United Kingdom.
- Bailis, R., R. Drigo, A. Ghilardi, and O. Masera. 2015. The carbon footprint of traditional wood fuels. *Nature Climate Change*, 5(3): 266-272.
- Bantelay, D. T., and N. Gabbiye. 2014. Design, manufacturing, and performance evaluation of household gasifier stove: A case study of Ethiopia. *American Journal of Energy Engineering* 2(4): 96-102.
- Bello, R. S., M. A. Onilude, and T. A. Adegbulugbe. 2015. Design and performance evaluation of supplemental air supplied charcoal stove. *International Letters of Chemistry, Physics and Astronomy*, 54: 1-10.
- Belonio, A. T. 2005. Rice husk gas stove handbook. Iloilo city, Philippines: Department of agricultural engineering and environmental management, college of agriculture, central Philippine University.
- Boafo-Mensah, G., K. Ampomah-Benefo, M. A. B. Animpong, W. O. Oduro, E. N. Kotey, K. Akufo-Kumi, and G. N. Laryea. 2013. Thermal efficiency of charcoal-fired cookstoves in Ghana. *Global Advanced Research Journal of Engineering, Technology, and Innovation*, 2(3): 102-110.
- Boafo-Mensah, G., K. M. Darkwa, and G. Laryea. 2020. Effect of combustion chamber material on the performance of an improved biomass cookstove. *Case Studies in Thermal Engineering*, 21: 100688.
- Bryden, M., D. Still, P. Scott, G. Hoffa, D. Ogle, R. Bailis, and K. Goyer. 2005. *Design Principles for Wood Burning Cook Stoves*. 80574 Hazelton Road, Cottage Grove : Aprovecho Research Center
- Bureau of Indian Standards (BIS). 2013. Solid biomass chulha specifications (BIS 13152, Part 1). New Delhi, India: Indian

- Standard Institute.
- Capareda, S. C. 2011. Biomass energy conversion. In *Sustainable Growth and Applications in Renewable Energy Sources*, eds. M. Nayeripour, and M. Kheshti, ch. 10, 209-226. Amazon.com: Books on Demand .
- Castaner, M., D. Li, and N. Minor. 2017. An efficient and safe cooking for Las Delicias, El Salvador. Senior Design Report 92. Philadelphia, PA, USA: Department of Chemical and Biomolecular Engineering, University of Pennsylvania.
- Chen, Y., D. Pew, and D. Abbott. 2018. Cookstove efficiency, health, and environmental impacts. Biomass Lab Report. Portland, Oregon: TR Miles Technical Consultants Inc.
- Global Alliance for Clean Cookstoves (GACC). 2017. Handbook for biomass cookstove research, design, and development. A *Practical Guide to Implementing Recent Advances. D-Lab*. 1-52. www.cleancookstove.org
- Gumino, B., N. A. Pohlman, J. Barnes, and P. Wever. 2020. Clean technologies design features and performance evaluation of natural-draft, continuous operation gasifier cookstove. *Clean technology*, 2(3): 252-269.
- Keche, A. J., G. A. P. Rao, and R. G. Tated. 2013. Effective utilization of low-density biomass in a downdraft gasifier. *International Journal of Ambient Energy*, 7(3): 27-33.
- Komolafe, C. A., and O. Awogbemi. 2010. Fabrication and performance evaluation of an improved charcoal cooking stove. *The Pacific Journal of Science and Technology*, 11(2): 51-58.
- Kulla, D. M. 2011. Technology improvement for safety and economy in wood burning devices in Nigeria. Ph.D. diss., Department of Mechanical Engineering, Ahmadu Bello University Zaria, Nigeria.
- Kumar, H., and N. L., Panwar (2019). Experimental investigation on energy-efficient twin-mode biomass improved cookstove. *SN Applied Sciences*, 1(7): 1-8.
- Mehetre, S. A., N. L. Panwar, D. Sharma, and H. Kumar. 2017. Improved biomass cookstoves for sustainable development: A review. *Renewable and Sustainable Energy Reviews*, 73: 672-687.
- Odesola, I. F., and A. O. Kazeem. 2014. Design, construction, and performance evaluation of a biomass cookstove. *Journal of Emerging Trends in Engineering and Applied Sciences*, 5(5): 358-362.
- Omini, N. J. 2018. Design, construction, simulation, performance evaluation and emissions characterization of a rocket stove. M.S. thesis, Department of Mechanical Engineering, Ahmadu Bello University Zaria, Nigeria.
- Pal, R. K. 2016. Efficient use of biomass in improved cookstoves. *Journal of Engineering Science and Technology*, 11(12): 1808-1817.
- Patil, S. R., S. R. Kalbande, and V. P. Khambalkar. 2017. Feasibility evaluation of briquette biomass cook stove for rural area. *International Journal of Current Microbiology and Applied Sciences*, 6(10): 3190-3203.
- Rupnar, A., and P. Chauhan. 2016. Design, development of domestic cookstove suitable for different solid biomass fuel. *International Journal of Environment, Ecology, Family, and Urban Studies*, 6(6): 15-22.
- Saiyyadjilani, S. S., P. G. Tewari, R. Tapaskar, A. P. Madival, M. Gorawar, and P. P. Revankar. 2018. Design of improved biomass cook stove for domestic utility. *International Conference on Advanced Technologies for Societal Applications*, eds P. Pawar, B. Ronge, R. Balasubramaniam, and S. Seshabhattar, 53-63. Techno-Societal: Springer International Publishing AG.
- Solapure, V. R., N. S. Motgi, and Y. N. Jangale. 2017. Design and performance analysis of biomass cook stove. *International Journal of Engineering Research and Technology*, 6(7): 296-300.
- Sood, S. P., Y. P. Khandetod, A. G. Mohod, R. M. Dharaskar, and K. G. Dhande. 2018. Development and evaluation of biomass cookstove. *Advanced Agricultural Research & Technology Journal*, 2(1): 76-80.
- Thomson, D., J. Couburn, W. Sanchez, A. Laurent, and C. C. Microsol. 2016. Increasing commitments to clean-cooking initiatives. Gold Standard Improved Cookstove Activities Guidebook. Avenue Louis Casai 79 CH-1216, Geneva-Cointrin, Switzerland: Gold Standard Foundation.
- Usman, O. Y. 2011. Experimental performance evaluation of charcoal- stove. Unpublished M.S. thesis, University of Nigeria, Nsukka.
- Wilson, D. L., D. R. Talancon, R. L. Winslow, X. Linares, and A. J. Gadgil. 2016. Avoided emissions of a fuel-efficient biomass cookstove dwarf embodied emissions. *Development Engineering*, 1: 45-52.
- World Health Organization (WHO). 2021. Household air pollution and health. Avenue Appia 20 1211 Geneva 27 Switzerland: WHO.